J Intell Robot Syst
DOI 10.1007/s10846-013-0013-6

Enhanced PCA-Based Localization Using Depth Maps with Missing Data

Experimental Validation

Fernando Carreira · João M. F. Calado · Carlos Cardeira · Paulo Oliveira

Received: 5 July 2013 / Accepted: 23 December 2013

Abstract In this paper a new method for self-localization of mobile robots, based on a PCA positioning sensor to operate in unstructured environments, is proposed and experimentally validated. The proposed PCA extension is able to perform the eigenvectors computation from a set of signals corrupted by missing data. The sensor package considered in this work contains a 2D depth sensor pointed upwards to the ceiling, providing depth images with missing data. The positioning sensor obtained is then integrated in a Linear Parameter Varying mobile robot model to obtain a self-localization system, based on linear Kalman filters, with globally stable position error estimates. A study consisting in adding synthetic random corrupted data to the captured depth images revealed that this extended PCA technique is able to reconstruct the signals, with improved accuracy. The self-localization system obtained is assessed in unstructured environments and the methodologies are validated even in the case of varying illumination conditions.

Keywords Mobile robots · Robot sensing systems · Sensor fusion · Principal component analysis · Kalman filters

F. Carreira (✉) · J. M. F. Calado · C. Cardeira · P. Oliveira
IDMEC/LAETA - Instituto Superior Técnico, Universidade de Lisboa, Av. Rovisco Pais 1, 1049-001 Lisboa, Portugal
e-mail: fcarreira@dem.isel.pt

J. M. F. Calado
e-mail: jcalado@dem.isel.pt

C. Cardeira
e-mail: carlos.cardeira@tecnico.ulisboa.pt

P. Oliveira
e-mail: p.oliveira@dem.ist.utl.pt

F. Carreira · J. M. F. Calado
ADEM - Instituto Superior de Engenharia de Lisboa, Instituto Politécnico de Lisboa, R. Conselheiro Emídio Navarro, 1, 1959-007 Lisboa, Portugal

P. Oliveira
ISR/LARSyS - Instituto Superior Técnico, Universidade de Lisboa, Av. Rovisco Pais 1, 1049-001 Lisboa, Portugal

1 Introduction

The problem of mobile robots localization with only onboard sensors in indoors environments has been a great challenge to researchers in mobile robotics, see [3, 11] and the references therein. To perform this task, usually, mobile robots are equipped with different types of sensors like compasses, accelerometers, gyros, cameras, time of flight cameras and encoders, providing enough information to the measuring system to determine its global pose, i.e., position and orientation in a mapped environment.

Published online: 24 January 2014

Vision is one of the most popular sensors in mobile robotics to provide measurements to solve the localization, due to the large amount of information provided on the environment, extracted from the RGB image [14, 19, 24, 28]. However, in vision systems remains a general limitation related to different environment lighting conditions that decreases the localization systems robustness.

To avoid the above mentioned problem, some localization systems are based on time-of-flight sensors [20]. The use of time-to-flight sensors allows the acquisition of depth information about the environment and presents a more robust system able to cope with different light conditions. Moreover, the time-of-flight cameras allow the capture of depth images, where the sensor is able to receive a grid with depth information from all field of view [1]. However, it is expensive to implement this type of cameras in many mobile robotic platforms.

Recently, the companies PrimeSense and Microsoft developed a device primarily for video games, denominated as Kinect, that combines a RGB and a depth camera. Due to its low price and a straightforward way to be connected with a computer, the Kinect device became popular in mobile robotics community creating several different applications of mobile robots. In [4, 10], mobile robot navigation systems are proposed, based on data acquired by a Kinect sensor. Also, Kinect depth images are central for a wheelchair localization system reported in [27]. The combination of RGB and depth images are also used, see [13, 15, 26] for details. However, these works are based on EKF and particle filters, with the well-known stability issues.

A very common problem in depth sensors, including the Kinect depth sensor, is the existence of missing data in signals, caused by IR (infrared) beams that are not well reflected, not returning to the depth sensor receiver. In [23], a method using the Principal Component Analysis (PCA) methodology is presented to avoid the problem of missing data in signals and its performance is compared with other state-of-the-art algorithms, concluding that the PCA algorithm can be extended to reconstruct signals corrupted with missing data, and presents a better performance (less interpolation error) in an extended range of missing data. The PCA [17] is an efficient algorithm that converts the database into an orthogonal space creating a database with a high compression ratio, when compared with the amount of captured data. Moreover, the PCA allows to develop localization systems that do not depend on any predefined structure [2, 18], i.e, does not need to detect any specific features about the environment. In [22], PCA is used for terrain reference navigation of underwater vehicles.

There are different approaches in installing cameras to develop localization systems. The most common solution is to allow placement of cameras to look around obtaining the corresponding position [4, 14, 21, 25], while some mobile robots use a single camera looking upward [12, 16, 30]. Ceiling-based visual positioning has the advantage that images can be considered without scaling and are static. This approach was successfully implemented in [6, 9]. In general, the transformation that relates two images obtained by a mobile robot, to estimate its motion, is a perspective projection based in the pinhole camera model. Ceiling-based visual positioning has the advantage that, under the planar scene assumption and assuming that the camera is orthogonal to the ceiling plane, the image transformation to relate two images is defined by just three parameters, a 2D translation and one rotation. Moreover, the static scenario assumption is usually valid for images of the ceiling.

While many localization systems uses the information of extraction features to the localization of the mobile robot in a structured environment [4, 16, 21], the use of PCA allows the creation of a localization system, in an unstructured environment, with a great compression ratio and without the need of specific feature extracting.

In this work, the main purpose is the experimental validation of [23], resorting to a mobile robot self-localization system, using depth images corrupted with missing data. The implemented position sensor is based on an extension of the PCA algorithm able to reconstruct corrupted signals through the orthogonal space, which is fused in a Linear Parameter Varying model, resorting to a sub-optimal linear Kalman filter. This approach presents advantages relative to the usual EKF solution that in general has no guarantees of stability, due to incorrect estimates used on the linearization [7].

This paper is organized as follows: Section 2 presents the mobile robot platform and the motivation for the use of Kinect in the proposed localization system. In Section 3 the principal component analysis

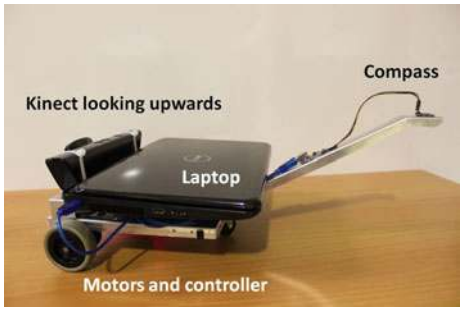

Fig. 1 Mobile platform equipped with kinect sensor and compass

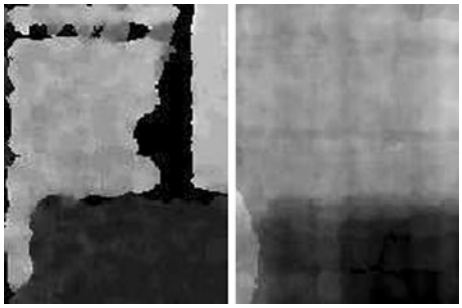

Fig. 3 Captured depth image with corrupted data (*left*) and reconstructed through PCA (*right*)

for signals with missing data is detailed. For performance analysis purposes, Section 4 presents experimental depth image reconstruction results, using the PCA algorithm for signals corrupted with different ratios of missing data. In Section 5, an architecture for mobile robot self-localization, composed by PCA and Kalman filters is introduced, and the experimental results for localization with missing data, estimation stability, and localization in repeatability scenarios is presented. Finally, Section 6 presents some conclusions and unveils future work.

2 Model Platform

The experimental validation of the positioning system proposed in this paper is performed resorting to a low cost mobile robotic platform [5], with the configuration of a Dubins car. A Microsoft Kinect is installed on the platform, pointing upwards to the ceiling, together with a digital compass, located on the extension arm (robot rear part) to avoid the magnetic interference from the motors, as depicted in Fig. 1.

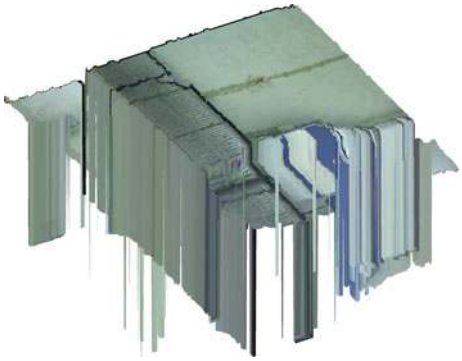

Fig. 2 RGB-D image of the ceiling view obtained by the kinect installed onboard the mobile robot

The Kinect includes a RGB camera with a VGA resolution (640 × 480 pixels) using 8 bits and a 2D depth sensor (640 × 480 pixels) with 11 bits of resolution. The use of this sensor for mobile robots localization could combine the capture of a RGB image and a depth map about the environment, obtaining RGB-D images, as shown in Fig. 2. This image depicts the ceiling view captured by the Kinect installed onboard the mobile robot. Note that it is possible to observe both the 3D shape of the existing technical installations in the ceiling and its color.

The robot moves indoors, in buildings with some information (e.g. building-related systems such as HVAC, electrical and security systems, etc.). It is possible to use the signals captured by a Kinect looking upward (RGB image, depth map or both) by an algorithm that can provide mobile robot global position in the environment.

Due to limitations found in image-based mobile robot localization approaches, regarding lighting changes, and aiming the development of an efficient self-localization solution that can work in places with uncontrolled lighting changes, only the Kinect depth signal is used, resorting to an adaptation to the method proposed in [6–8, 22] to the problem at hand.

However, as it is possible to observe in Fig. 2, due to geometry and properties of some objects, that several waves are not well reflected and, thus, can not be detected by the depth sensor receiver. In the case of Kinect, such a problem results in the existence of points with null distance (0 mm) inside the data array with the depth values (distances to various points in the plane), that may lead to erroneous results in the localization system. In this paper an extension of a

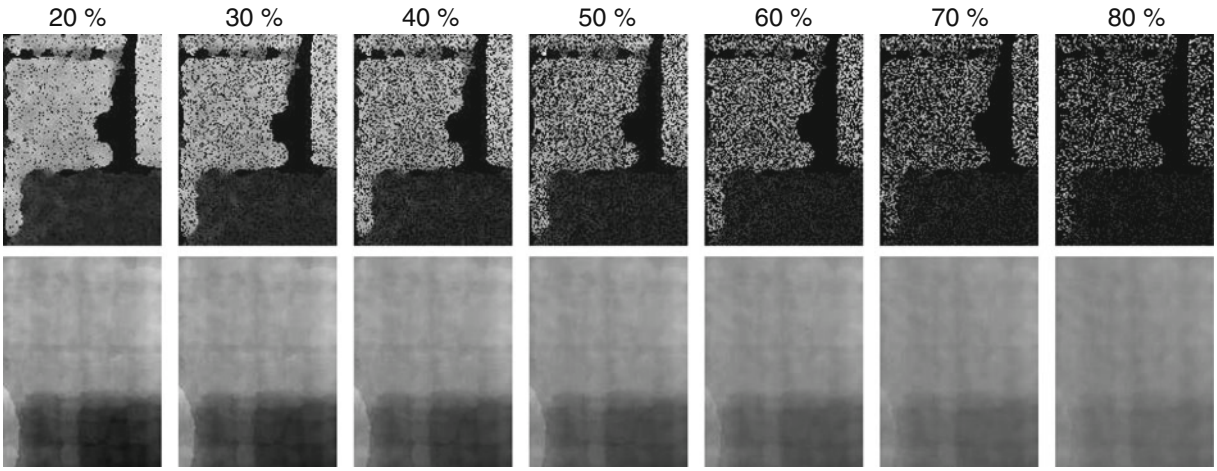

Fig. 4 Captured depth image with added corrupted data (*top*) and reconstructed through PCA (*bottom*)

PCA-based position approach will be presented aiming to cope with lighting changes common to usual vision systems, to be experimentally validated.

3 PCA for Signals with Missing Data

PCA [17] is a methodology based on the Karhunen-Loève (KL) transformation that is often used in applications that need data compression, like image and voice processing, data mining, exploratory data analysis and pattern recognition. The data reduction is obtained through the use of a database eigenspace approximation by the best fit eigenvectors. This technique makes the PCA an algorithm that has a high compression ratio and requires reduced computational resources. The PCA algorithm is used as the mobile robot position sensor in [7, 8].

The PCA eigenspace is created based on a set of M stochastic signals $\mathbf{x}_i \in \mathbb{R}^N,\ i = 1, \ldots, M$ acquired by a Kinect depth sensor installed onboard the mobile robot, considering an area with M mosaics in two dimensional space, $N = N_x N_y$, where N_x and N_y are the number of pixels in x and y axis of each mosaic, respectively.

In the common PCA-based approaches, the eigenspace of the set of acquired data is characterized by the corresponding mean $\mathbf{m}_x = \frac{1}{M}\sum_{i=1}^{M} \mathbf{x}_i$ and covariance $\mathbf{R}_{xx} = \frac{1}{M-1}\sum_{i=1}^{M} (\mathbf{x}_i - \mathbf{m}_x)(\mathbf{x}_i - \mathbf{m}_x)^T$. However, the existence of missing data in signal $\mathbf{x}_i$ corrupts the PCA mean value computation creating an orthogonal space with erroneous data.

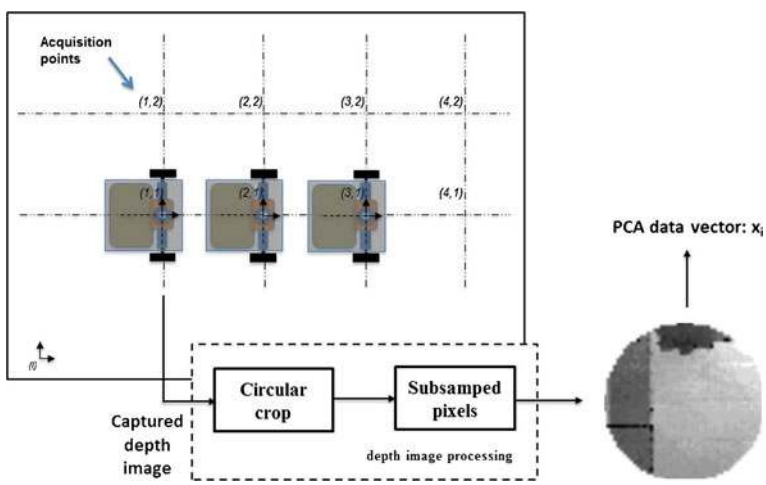

Fig. 5 Grid map and depth image processing to create a PCA eigenspace

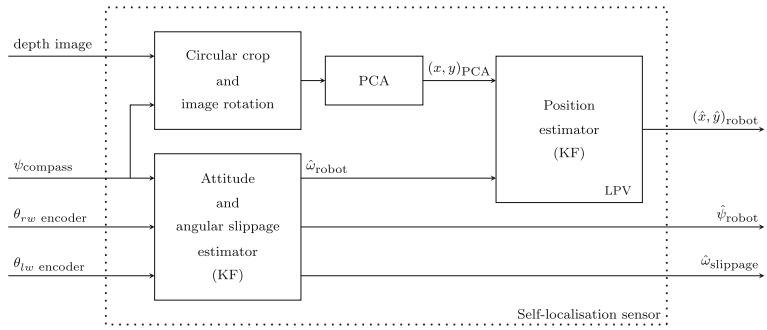

Fig. 6 Architecture of the self-localization sensor

In the case where missing data occurs, the classical approach to compute the covariance matrix, resorts to a mean substitution operation. Thus, a vector $\mathbf{l}$ with length N consisting of boolean values is used to mark the real and missed data of a signal $\mathbf{x}_i$. Then, considering the jth component of acquired signal $\mathbf{x}_i$, the index $\mathbf{l}_i(j)$ is set to 1 if the signal $\mathbf{x}_i(j)$ is available and it is set to 0 if there is a missing data.

Hence, to avoid the negative impact of the sensor signals missing data in PCA-based approaches performance, an extension to this methodology is proposed in this paper, where instead of considering all values of the M stochastic signals to compute the previously mentioned, only the correct data is used to compute the orthogonal space, characterized by $\mathbf{m}_x$ and $\mathbf{R}_{xx}$, and the value corresponding to missing data is neglected. Thus, the auxiliary counters $\mathbf{c} = \sum_{i=1}^{M} \mathbf{l}_i$ and $\mathbf{C} = \sum_{i=1}^{M} \mathbf{l}_i \mathbf{l}_i{}^T$ are defined, based on the auxiliary vector $\mathbf{l}$ defined before.

Considering the set with M signals, the mean ensemble for the jth component is given by:

$$\mathbf{m}_x(j) = \frac{1}{c(j)} \sum_{i=1}^{M} \mathbf{l}_i(j)\mathbf{x}_i(j), \quad j = 1, ..., N \tag{1}$$

and the covariance element $\mathbf{R}_{xx}(j,k), \quad \{j,k\} = 1, ..., N$ is computed as follows:

$$\mathbf{R}_{xx}(j,k) = \frac{1}{C(j,k) - 1} \sum_{i=1}^{M} \mathbf{l}_i(j)\mathbf{l}_i(k)\mathbf{y}_i(j)\mathbf{y}_i(k) \tag{2}$$

where $\mathbf{y}_i = \mathbf{x}_i - \mathbf{m}_x$.

Considering the new mean ensemble and covariance of the PCA database computed without corrupted data in (1) and (2), the decomposition into the orthogonal space follows the PCA algorithm classical approach, i.e. $\mathbf{v} = \mathbf{U}^T(\mathbf{x} - \mathbf{m}_x)$. The matrix $\mathbf{U} = [\mathbf{u}_1 \ \mathbf{u}_2 \ \ldots \ \mathbf{u}_N \ ]$ should be composed by the N orthogonal column vectors of the basis, verifying the eigenvalue problem:

$$\mathbf{R}_{xx}\mathbf{u}_j = \lambda_j \mathbf{u}_j, \quad j = 1, ..., N, \tag{3}$$

Matrix $\mathbf{R}_{xx}$ has a size of $N \times N$. As there are M images there are at most $M - 1$, rather than N^2, meaningful eigenvectors. The remaining eigenvectors of $\mathbf{R}_{xx}$ will have associated eigenvalues of zero. As $M < N$, the $M - 1$ eigenvectors may be efficiently computed using Turk and Pentland method [29].

Assuming that the eigenvalues are ordered, i.e. $\lambda_1 \geq \lambda_2 \geq \ldots \geq \lambda_N$, the choice of the first $n \ll N$ principal components leads to stochastic signals approximation given by the ratio on the covariances associated with the components, i.e. $\sum_n \lambda_n / \sum_N \lambda_N$.

Although a trade-off between the PCA discrimination and the data compression ratio can be observed, in the selection of the number of principal components, its relationship is non-linear. Thus, selecting only a few principal components, it is possible to achieve a high variability of the eigenspace, even with high compression ratio. A larger number of eigenvectors would provide minimal performance improvement, with an increase of memory required.

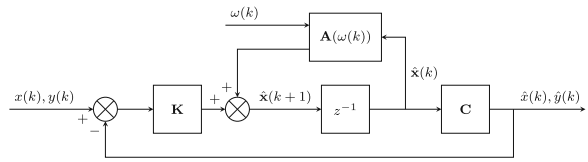

Fig. 7 Block diagram of the position estimator

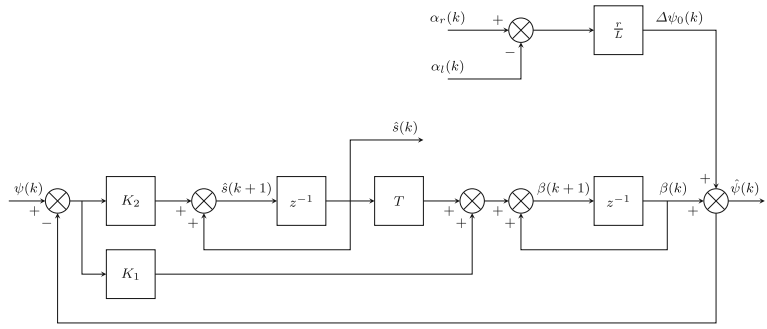

Fig. 8 Block diagram of the attitude and angular slippage estimator

4 PCA-Based Depth Image Reconstruction

As mentioned in the Section 2, the self-localization system proposed in this paper uses depth images corrupted with missing data, captured from the ceiling. Thus, to validate the concept of the image reconstruction resorting to a PCA eigenspace, a test of reconstructing a depth image corrupted with missing data is performed.

In order to create the PCA eigenspace, a set of 125 depth images are captured along a grid map with a distance of 0.3 m (in x and y axis) in an area of 5 $m \times 4.5$ m. Considering that the Kinect depth sensor has a resolution of 640 by 480 points, and with the purpose of reducing the amount of data stored in PCA eigenspace, the depth images are cropped to a depth image with 120 by 160, extracting the central area of the images, and transforming them into vectors $\mathbf{x}_i \in \mathbb{R}^{19200}$, $i = 1, \ldots, 125$.

In order to test the depth image reconstruction using the proposed extension of the PCA algorithm, a new depth image is captured from the ceiling, corrupted with about 15 % of missing data ratio. The depth image is shown in left side of Fig. 3, where the black pixels correspond to the missing data. Applying the proposed algorithm, the depth image reconstruction is performed, decomposing the captured corrupted signals into the orthogonal space, obtaining the corresponding loading, according to the following steps:

1. identify the non-corrupted data in the vector $\mathbf{l}$;
2. build the auxiliary counters $\mathbf{c}$ and $\mathbf{C}$;
3. substitute the corrupted data $\mathbf{x}_i(j)$ by the corresponding mean $\mathbf{m}_x(j)$;

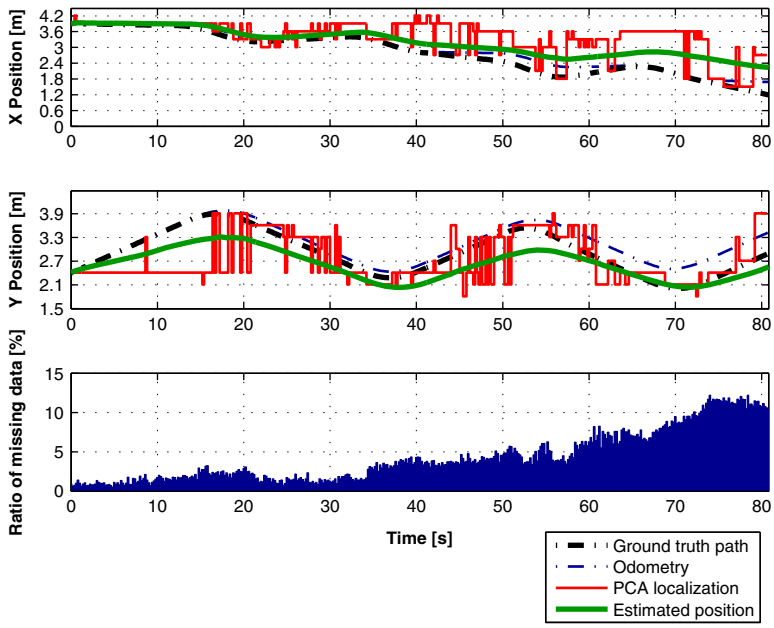

Fig. 9 Estimated position along time without corrupted data correction

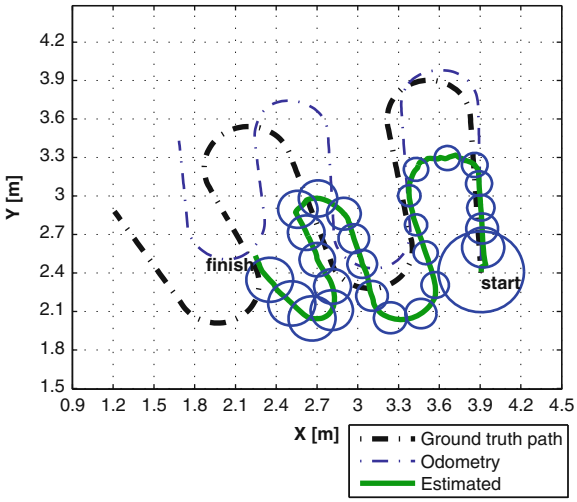

Fig. 10 Map with estimated position considering a ground truth path, without corrupted data correction

4. decompose the signal after the mean substitution into the orthogonal eigenspace **v**;
5. compute the reconstructed depth image recovering the signals from the eigenspace computed before.

Analyzing the depth images in Fig. 3, it is possible to conclude that the PCA is able to construct a similar depth image (right), removing all corrupt pixels present in the original captured image (left). It is also possible to observe that the pixels with non corrupted data are not equal to the captured depth image. However, in this case, the PCA algorithm is performing tree important tasks at same time: i) compression of the acquisition database; ii) removing the corrupted data of the depth image; iii) and creating a eigenspace to compare the reconstructed depth image with the PCA database, without explicit features extraction.

To analyze robustness of the corrupted depth image reconstruction technique proposed, a new test is performed, removing depth information from the acquired data. The depth image reconstruction using PCA is simulated, adding from 20 % to 80 % random missing data. Figure 4 shows the captured depth images with the added missing data on the top, and the reconstructed images at the bottom. Analyzing the results it is perceptible that the reconstruction of the depth image, by the proposed PCA algorithm, provides good results until a missing data ratio of about 60 %. Further details on the reconstruction accuracy will be presented next. However, observing the corrupted depth images, it is possible to see that for higher ratios of missing data, there is too much degradation to reconstruct the corrupted image.

5 Concept Validation in 2D Localization

In order to solve the problem of 2D mobile robot localization, a new PCA eigenspace is created with a

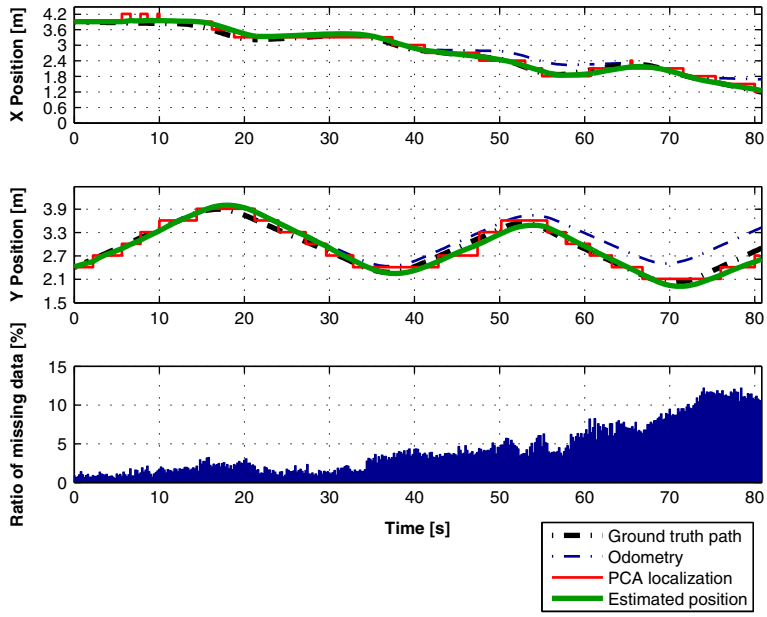

Fig. 11 Estimated position along time

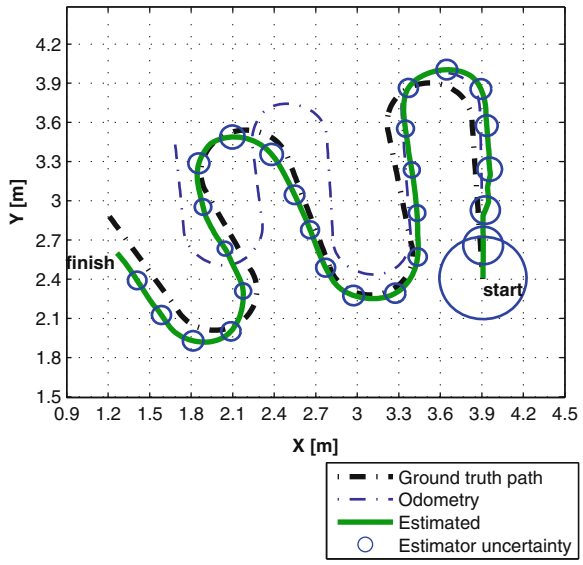

Fig. 12 Map with estimated position considering a ground truth path

set of captured depth images along a grid map with a distance of 0.3 m (in x and y axis) in an area of 5 $m \times 4.5$ m. This is a manual process to ensure that all images are captured in the same direction and the depth sensor is in the right grid position (Fig. 5). The captured depth images are cropped with a circular mask allowing the rotation and comparison of captured depth images when the robot is in the same position, but with different attitude, during a mission.

In order to compress the amount of data, the depth images are sampled with a compression ratio of 100 : 1 and converted into a vector that will be added to PCA eigenspace. In [6, 7], the authors followed a similar approach using a RGB camera, but the method revealed to be sensitive to lighting changes.

During the mission, the signal $\mathbf{x}$ is decomposed into the orthogonal space considering only the non-corrupted data. Thus, before the projection of the depth image into the orthogonal space, the mean substitution should be followed, i.e, all jth component of the signal $\mathbf{x}_i$ with corrupted data should be replaced by the corresponding mean value $\mathbf{m}_x(j)$. This method removes the effect of the corrupted data in its decomposition in the orthogonal space $\mathbf{v} = \mathbf{U}^T(\mathbf{x} - \mathbf{m}_x)$.

The robot position $\hat{x}$ and $\hat{y}$ is obtained by finding a given neighborhood δ, the mosaic whose eigenvector is nearest to the acquired signal decomposed into the orthogonal space:

$$\forall_i \|[\hat{x}\,\hat{y}]^T - [x_i\, y_i]^T\|_2 < \delta, r_{\text{PCA}} = \min_i \|\mathbf{v} - \mathbf{v}_i\|_2; \quad (4)$$

Given the mosaic i that verifies this condition, its center coordinates $[x_i\ y_i]^T$ are selected as the robot position, obtained by the PCA-based sensor.

Then, the mean substitution approach is used when there is missing data in the depth signals coming from the Kinect sensor. Just like during the creation of the PCA eigenspace, it must be done before the application of the PCA algorithm, i.e., all jth component of

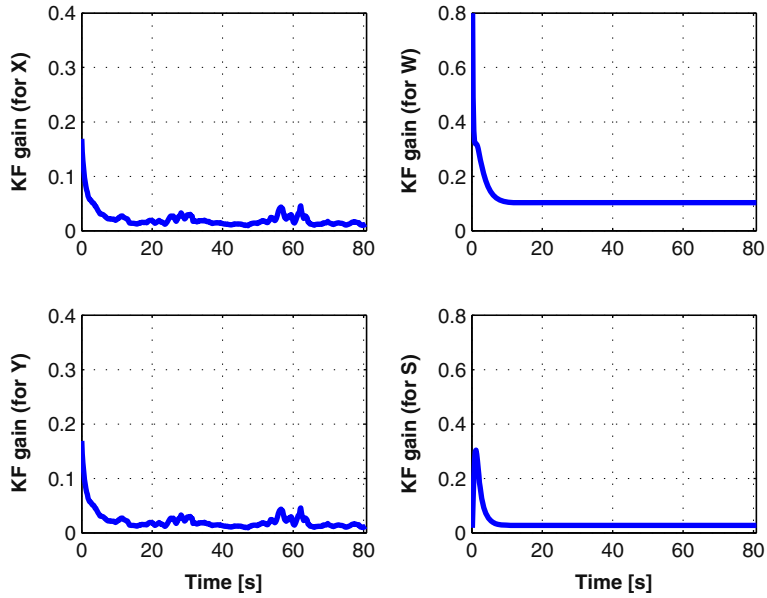

Fig. 13 Evolution of the Kalman filter gains: position estimator (*left*) and attitude estimator (*right*)

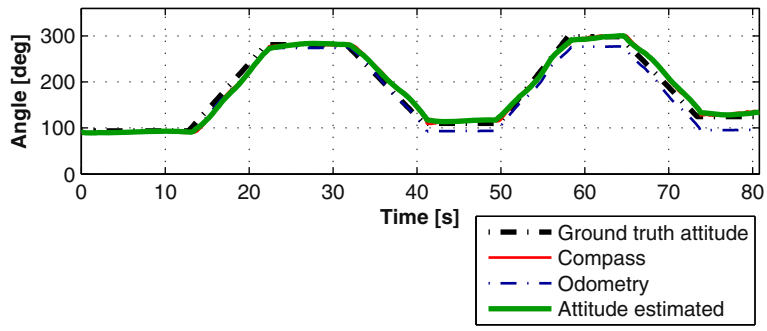

Fig. 14 Evolution of the attitude estimated considering a ground truth path

the signal $\mathbf{x}_i$ should be replaced by the corresponding mean value $\mathbf{m}_x(j)$.

During an experiment, the data captured from the sensors (Kinect, compass and encoders) has been used in a self-localization sensor based in two KF and one PCA algorithm, as detailed in Fig. 6. The implemented architecture allows the estimation of the robot attitude and position, as well as the angular motion speed and the robot angular slippage, using only the signals obtained by the onboard sensors.

The following notation is used in Fig. 6:

- $\psi_{compass}$ - orientation angle given by the compass;
- $\theta_{rwencoder}$ - angle given by the encoder of the right wheel;
- $\theta_{lwencoder}$ - angle given by the encoder of the left wheel;
- $(x, y)_{PCA}$ - coordinates given by the PCA sensor;
- $(\hat{x}, \hat{y})_{robot}$ - estimated robot coordinates in the world referential;
- $\hat{\omega}_{robot}$ - estimated angular speed;
- $\hat{\omega}_{slippage}$ - estimated differential slippage.

Detailing the architecture of the self-localization sensor presented in Fig. 6, the KF depicted on the left of the figure implements the attitude optimal estimator model that is responsible to estimate the mobile robot attitude and the angular slippage (see Section 5.2 for details). Once all acquired depth images for the PCA data-base are taken with the same orientation and compressed with a circular crop (Fig. 5), then, during a mission, the acquired depth images must be rotated to zero degrees of attitude, using the compass angle, and compressed with the same circular crop. The position estimator (on the right of the figure) implements a Linear Parameter-Varying (LPV) model as a function of the estimated angular speed in a KF, fusing it with the position obtained by the PCA algorithm (see Section 5.1 for details).

Resorting to this architecture, it is possible to estimate the position, attitude and angular slippage of the mobile robot with a global stable error dynamic. The next subsections shows the models and estimators implemented in this self-localization architecture. These models and estimators may be found, with more detail, in [7].

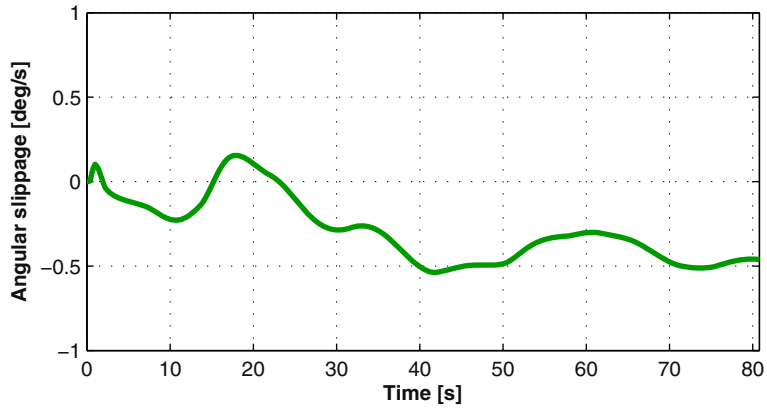

Fig. 15 Angular slippage estimated

5.1 Model for Position Estimation in 2D Localization

The classic differential drive mobile robot model is given by

$$\dot{x} = u\cos\theta \tag{5}$$

$$\dot{y} = u\sin\theta \tag{6}$$

$$\dot{\theta} = \omega \tag{7}$$

where u is the common mode speed, x and y are the robot coordinates in the world referential, θ is the orientation angle of the robot in the world referential and ω is the angular speed.

However, the classic non-linear model for differential drive mobile robots can be rewritten considering new state variables, becoming a Linear Parameter Varying (LPV) model. Thus, differentiating (5)–(7):

$$\ddot{x} = -u\,\omega\sin\theta = -\omega\dot{y} \tag{8}$$

$$\ddot{y} = u\,\omega\cos\theta = \omega\dot{x} \tag{9}$$

$$\ddot{\theta} = \dot{\omega} \tag{10}$$

and choosing as state vector $\mathbf{x} = [x\ \dot{x}\ y\ \dot{y}]^T$, a new LPV model for differential drive mobile robot is obtained:

$$\dot{\mathbf{x}} = \overbrace{\begin{bmatrix} 0 & 1 & 0 & 0 \\ 0 & 0 & 0 & -\omega \\ 0 & 0 & 0 & 1 \\ 0 & \omega & 0 & 0 \end{bmatrix}}^{\mathbf{A}} \mathbf{x} \tag{11}$$

$$\dot{\theta} = \omega \tag{12}$$

Considering the LPV model (11), (12) and assuming that ω is constant between two sampling times (zero order hold assumption), the follow discrete model can be obtained (see [7] for more details):

$$\mathbf{x}(k+1) = \overbrace{\begin{bmatrix} 1 & \frac{\sin\omega T}{\omega} & 0 & \frac{1}{\omega} + \frac{\cos\omega T}{\omega} \\ 0 & \cos\omega T & 0 & -\sin\omega T \\ 0 & \frac{1}{\omega} - \frac{\cos\omega T}{\omega} & 1 & \frac{\sin\omega T}{\omega} \\ 0 & \sin\omega T & 0 & \cos\omega T \end{bmatrix}}^{\mathbf{A}(\omega)} \mathbf{x}(k) + \underbrace{\begin{bmatrix} T & \frac{1-\cos\omega T}{\omega^2} & 0 & -\frac{\omega T - \sin\omega T}{\omega^2} \\ 0 & \frac{\sin\omega T}{\omega} & 0 & -\frac{1-\cos\omega T}{\omega} \\ 0 & \frac{\omega T - \sin\omega T}{\omega^2} & T & \frac{1-\cos\omega T}{\omega^2} \\ 0 & \frac{1-\cos\omega T}{\omega} & 0 & \frac{\sin\omega T}{\omega} \end{bmatrix}}_{\mathbf{G}(\omega)} \mu_{\mathbf{l}}(k) \tag{13}$$

$$\mathbf{y}(k) = \underbrace{\begin{bmatrix} 1 & 0 & 0 & 0 \\ 0 & 0 & 1 & 0 \end{bmatrix}}_{\mathbf{C}} \mathbf{x}(k) + \gamma_l(k) \tag{14}$$

where T is the sampling time, $\mu_{\mathbf{l}}$ is the discrete process noise based on the step invariant method used and γ_l is the noise present in the PCA position measurements, both assumed as zero-mean white Gaussian noise and uncorrelated.

Finally, in order to estimate the mobile robot position, the Linear Parameter Varying (LPV) model (13), (14) is fused with the position obtained by the PCA-based position sensor, through the KF presented in Fig. 7, where and $x(k)$ and $y(k)$ are the position obtained by the PCA sensor in instant k and $\hat{x}(k)$ and $\hat{y}(k)$ are the estimated position in the same instant.

5.2 Model for Attitude and Angular Slippage Estimation in 2D Localization

The model that describes the angular motion of the differential drive mobile robot is:

$$\dot{\psi} = \omega + s \tag{15}$$

$$\dot{s} = 0 \tag{16}$$

where ω is the angular speed, ψ is the attitude of the robot and s is the angular slippage in differential motion.

Considering the state vector $\theta = [\psi\ \ s]^T$, the kinematic model in state space can be defined by:

$$\dot{\theta} = \begin{bmatrix} 0 & 1 \\ 0 & 0 \end{bmatrix}\theta + \begin{bmatrix} 1 \\ 0 \end{bmatrix}\omega \tag{17}$$

Assuming that signals processing is performed by a digital processor, ω and ψ are constant between sampling times (zero order hold assumption), it is possible to obtain the discrete model of attitude:

$$\theta(k+1) = \overbrace{\begin{bmatrix} 1 & T \\ 0 & 1 \end{bmatrix}}^{\mathbf{A}}\theta(k) + \overbrace{\begin{bmatrix} T \\ 0 \end{bmatrix}}^{\mathbf{B}}\omega(k) + \overbrace{\begin{bmatrix} T & \frac{T^2}{2} \\ 0 & T \end{bmatrix}}^{\mathbf{G}}\mu_a(k) \tag{18}$$

$$y(k) = \underbrace{\begin{bmatrix} 1 & 0 \end{bmatrix}}_{\mathbf{C}}\theta(k) + \gamma_a(k) \tag{19}$$

where $\mu_{\mathbf{a}}$ is the discrete process noise and γ_a is the noise present in the compass measurements, both

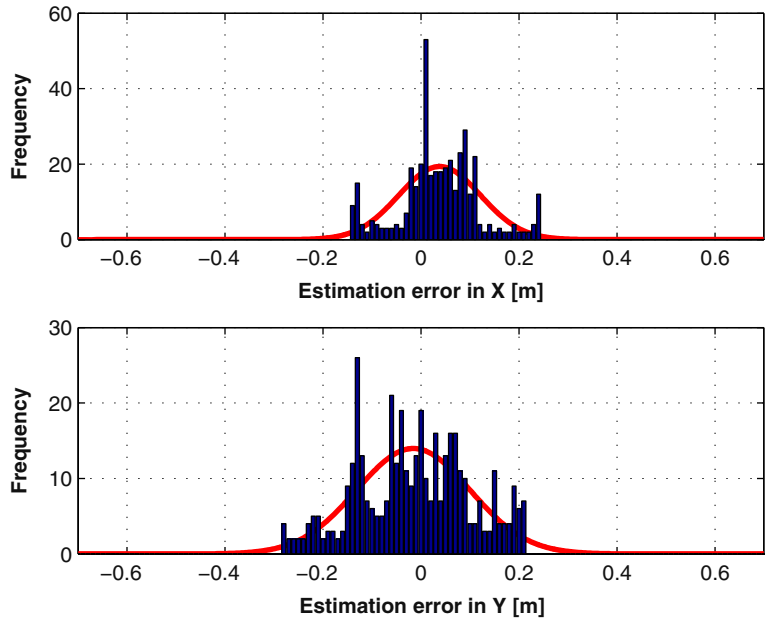

Fig. 16 Distribution of the estimated position error for both axis

assumed as zero-mean white Gaussian noise and uncorrelated.

Applying a KF to the discrete model (18), (19), following the steps described in [7], the optimal attitude and angular slippage estimator presented in Fig. 8 is obtained, where $\psi(k)$ is the angle of compass captured in instant k, r is the radius of the wheels, l is the distance between wheels, $\alpha_r(k)$ and $\alpha_l(k)$ are the lengths of the paths of left and right wheels (that can be read directly from the encoders onboard) and $\hat{\psi}(k)$ and $\hat{s}(k)$ are the estimated attitude and angular slippage of the robot, respectively.

Finally, the angular speed of the robot applied in LPV (14) is obtained through a numerical difference of the estimated attitude of the robot:

$$\hat{\omega}(k) = \frac{\hat{\psi}(k) - \hat{\psi}(k-1)}{T} \tag{20}$$

5.3 Results for 2D Localization with Classical PCA Algorithm

To observe the effect of corrupted data in the mobile robot self-localization, the depth images captured along the grid, after being subsampled and cropped with a circular mask, as presented before, are compressed using the classical PCA algorithm. The selection of the best eigenvectors is performing through eigenvalues that exceed 85 % of the total of the eigenvalues, creating an eigenspace with 60 eigenvectors.

To test the mobile robot self-localization performance of the proposed approach in a environment, several tests have been performed with the classical lawnmower type trajectory, combining both straight lines and curves, with a 0.1 m $\cdot$ s^{-1} robot speed and

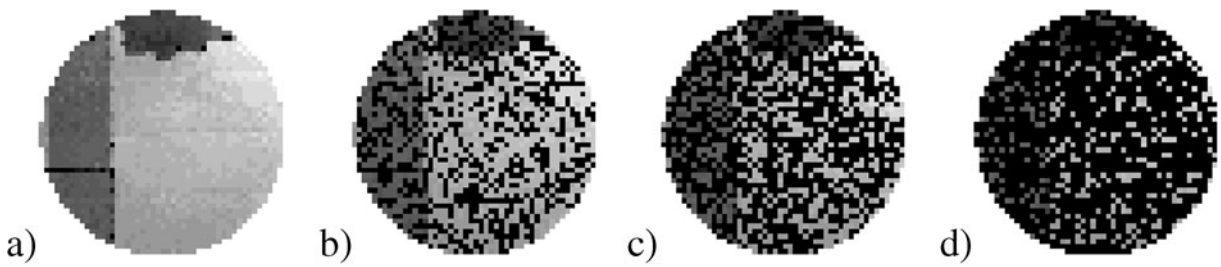

Fig. 17 First captured depth image: original **a**, and with added imposed corrupted data ratio to a ratio of 40 % **b**, 60 % **c** and 80 % **d**

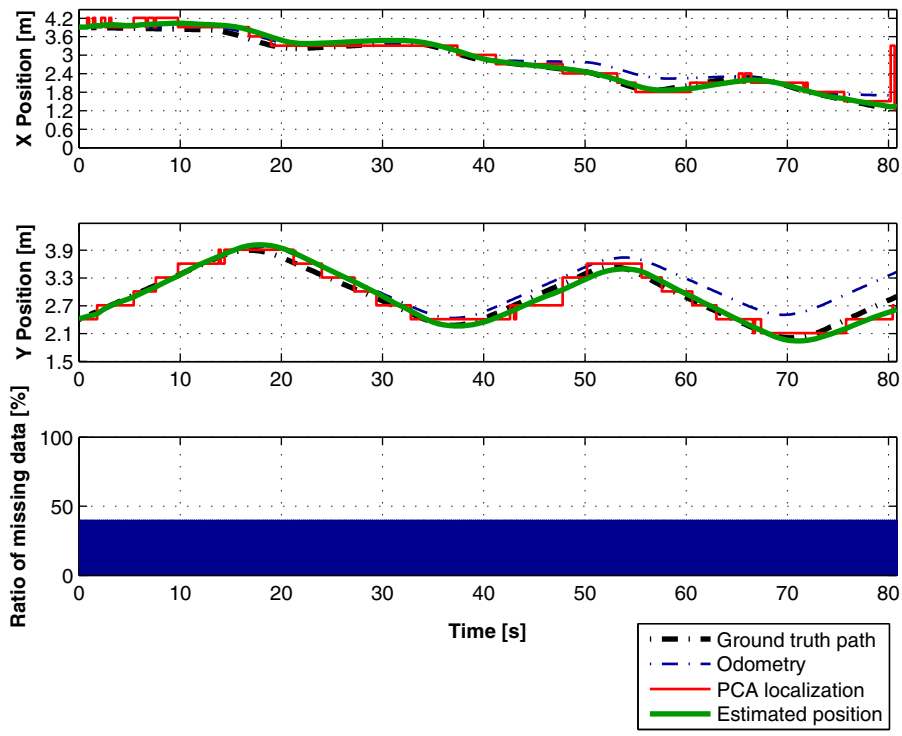

Fig. 18 Estimated position along time with 40 % of imposed corrupted data

5 Hz of sampling frequency. During the robot motion the real mobile robot trajectory has been measured allowing the comparison of the estimated position with the real one (ground truth test).

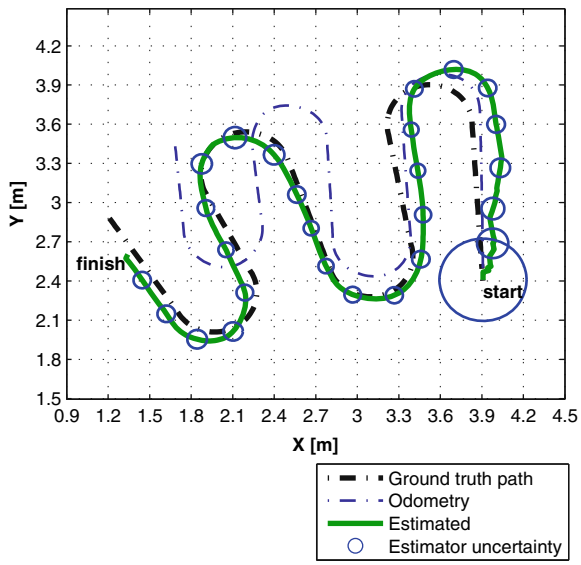

Fig. 19 Map with estimated position considering a ground truth path, with 40 % of imposed corrupted data

Analyzing Fig. 9 it is possible to see that, due the existence of missing data, the position obtained by the PCA algorithm often gives incorrect values, causing erroneous estimations in the self-localization system. Figure 10 shows the results of the PCA position sensor fused with the LPV model, in 2D localization. Analyzing Fig. 10, it is possible to conclude that the erroneous position obtained by the PCA, which is caused by the corrupted data, provides in the estimator a far localization than the described by the mobile robot (ground truth path).

5.4 Results for 2D Localization

Following the PCA algorithm extension proposed in Section 3, a new PCA eigenspace is created, computing the mean ensemble and the signals covariance, only with the non-corrupted data. Thus, choosing the best eigenvectors, which eigenvalues exceed 85 % of the total, an eigenspace with 30 eigenvectors is created.

As it is possible to see in Fig. 11, the position results obtained by the PCA algorithm is very close to the ground truth trajectory. Therefore, fusing the kinematic model of the robot with the position obtained by

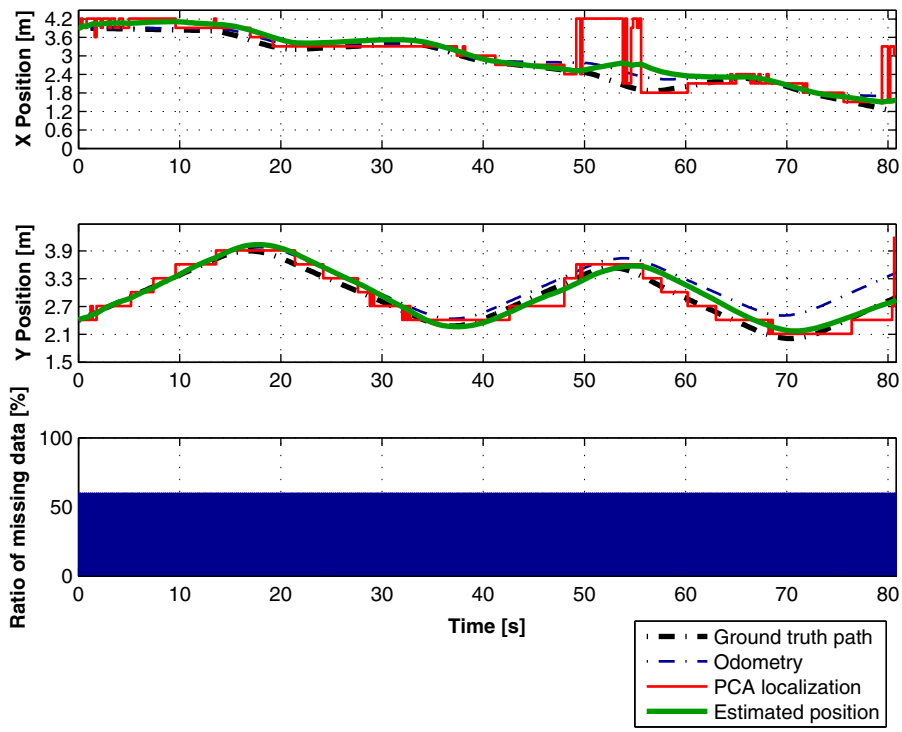

Fig. 20 Estimated position along time with 60 % of imposed corrupted data

PCA in the KF allows estimating position values with a very good accuracy.

Figure 12 shows the position estimated with the ground truth trajectory and the position obtained by the odometry. Comparing the results of the odometry with the estimated position it is possible to see an angular slippage in motion, that is increasing the difference between the estimated attitude and the one obtained by the odometry along time. This angular slippage is caused by systematic errors, such as uncertainties in the dimensions of the wheels, eccentric shaft problems, misalignment of the shafts, etc. It is possible to observe that in the initial part of the trajectory the estimator obtains a result close to the odometry. However, the localization system can approximate the estimated position with the ground truth trajectory.

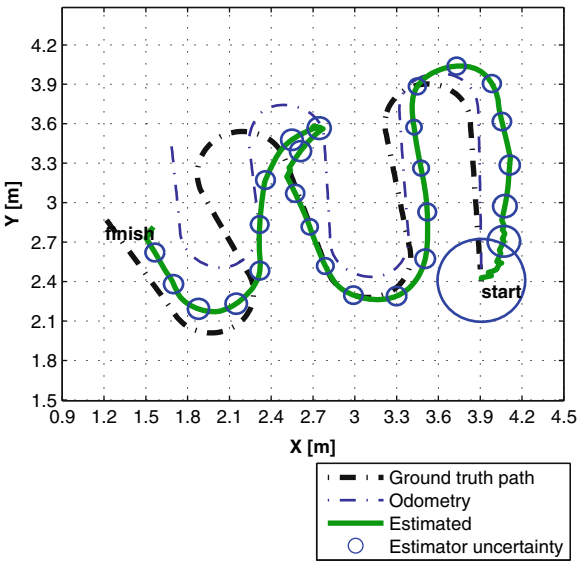

Fig. 21 Map with estimated position considering a ground truth path, with 60 % of imposed corrupted data

The Kalman gains stabilization along time are shown in Fig. 13, where it is possible to see that they converge in few sampling instants.

Analyzing the results of the attitude estimator in Fig. 14, it is possible to observe that the estimated attitude is very close to the ground truth, allowing to conclude that this Kalman filter provides results with good accuracy. Furthermore, analyzing Fig. 15, it is possible to observe the existence of an angular slippage of -0.5 rad $\cdot$ s^{-1} (positive for slippage in clockwise direction), that is detected at 40 s by the attitude estimator. Looking at Fig. 11 after 40 s (instant which is detected angular slippage), the results of the

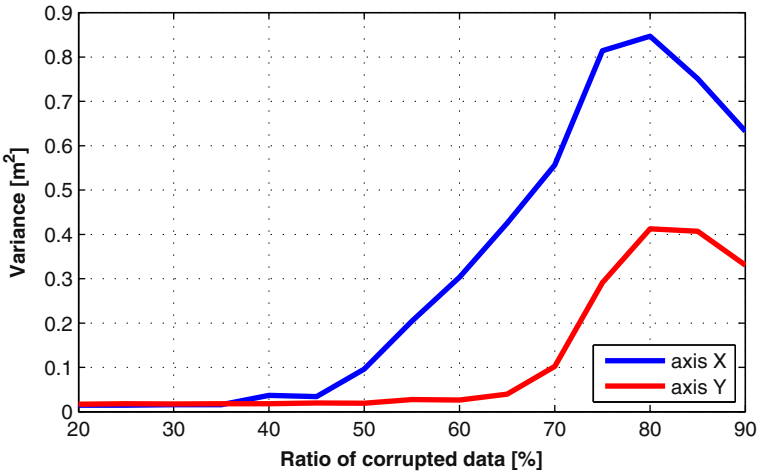

Fig. 22 Uncertainty of the PCA- based position sensor with corrupted data correction

position estimator are closer to the ground truth path than the odometry.

Finally, analyzing the histograms of Fig. 16, it is possible to conclude that the statistical distribution of the estimated position errors is approximately Gaussian with a mean close to zero. Moreover, comparing the variation of the distribution with the distance of the grid map acquired to create the PCA eigenspace (0.3 m), it is possible to see that, the proposed self-localization system is able to estimate the position with an error less than the distance between the acquired depth images.

5.5 Results for 2D Localization with Imposed Corrupted Data

The results presented in the previous section show the performance of the proposed algorithm in mobile robot localization considering depth images corrupted with missing data not exceeding 13 % (Fig. 11). The presence of the corrupted data in depth images is due to the geometry and properties of some objects that disturb several waves, causing the presence of the missing data. Therefore, as it is possible to observe in Fig. 11, the presence of corrupted data in the depth images is completely random.

Thus, in order to analyse the robustness of the proposed PCA algorithm in the presence of missing data, new self-localization tests are performed simulating depth images with missing data ration between 20 % and 90 %. For this test the same data captured from the sensors used in the previous Section is considered, but random corrupted data on the captured depth images is added. The amount and position of the missing data present in the captured depth images is analyzed, guaranteeing that the simulated corrupted data are randomly added in the non-corrupted data, keeping the same ratio in all depth images along the experiment. Figure 17 shows the original captured depth image in the initial position and the transformed data with the missing data added randomly to a ratio of 40 %, 60 % and 80 % of the signal length.

Analyzing the results, Fig. 18 shows that the proposed method is able to find depth image close to the captured along the travel, even with a ratio of 40 % corrupted data in all signals. Thus, the fusion of the

Table 1 Initial conditions of position and attitude stability validation in a lawn-mower trajectory

	x_0 [m]	y_0 [m]	ψ_0[°]
Robot position	3.9	2.4	90
Re-localization 1	4.4	2.4	0
Re-localization 2	4.4	1.9	315
Re-localization 3	2.9	1.6	225

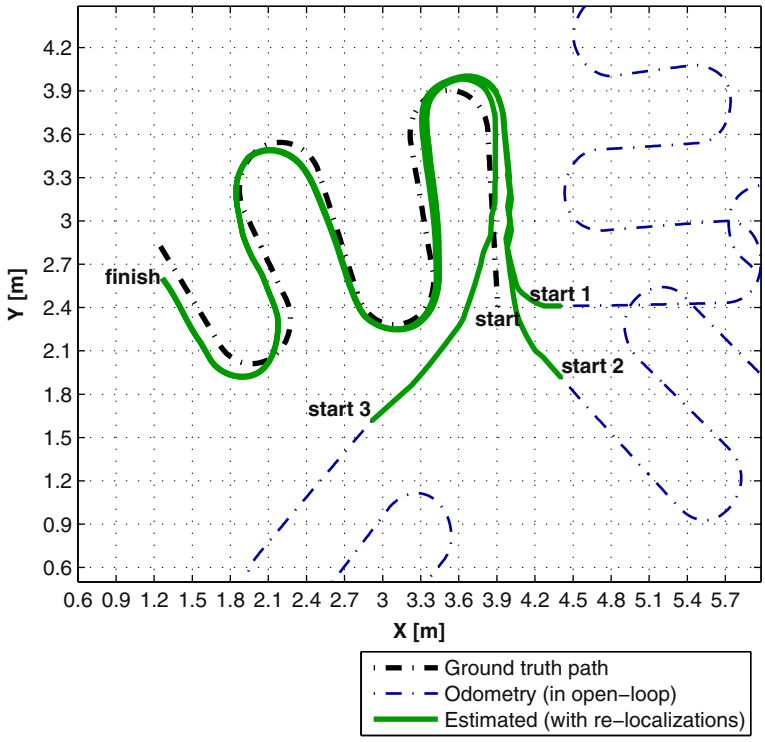

Fig. 23 Results of stability tests considering a wrong initial position and attitude estimates (map 2D)

PCA-based position with the KF allows the estimation with accuracy, presenting similar results to the obtained with the original data, where the ratio of missing data is less than 15 %, allowing the estimation with accuracy, after the stabilization of the angular slippage.

Analyzing the results using depth images with 60 % of missing data ratio presented in Fig. 20, it is possible to observe that the proposed algorithm is able to find the correct eigenvector in most of the acquired depth images. However, Fig. 20 also shows instants of time in which, given the large amount of data corrupted (see

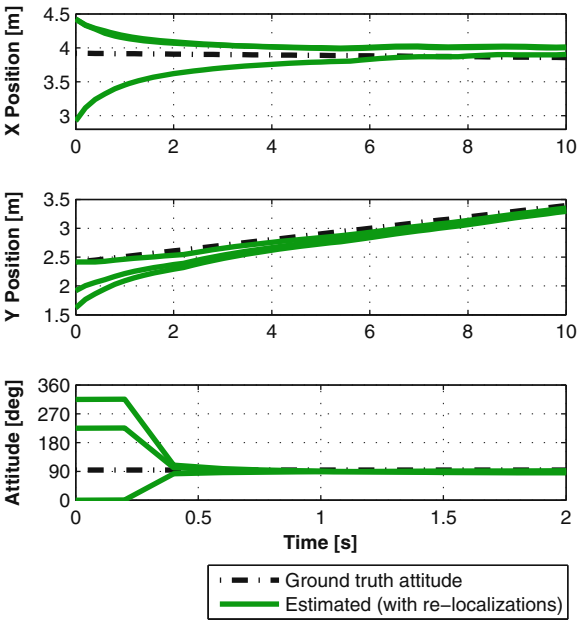

Fig. 24 Results of stability tests considering a wrong initial position and attitude (estimation along time)

Fig. 25 Ceiling view of the environment with periodic elements

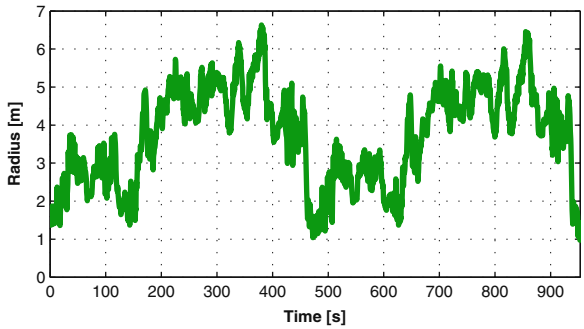

Fig. 26 Radius of searching neighborhood around the robot along time

Fig. 17), the algorithm found principal components similar to another captured image in a far location. This localization error, constant for several sampling times, led the KF to provide biased estimates, as it can be seen in Fig. 21.

Finally, Fig. 22 shows the estimation uncertainty of the PCA-based position sensor. As it is possible to observe, that the measurement accuracy is related to the ratio of corrupt data, but its relation is non-linear. The estimation uncertainty is equal in x and y coordinates to low ratio of corrupt data, while for high rations, the accuracy is different for both axis. Moreover, analyzing the results presented in Figs. 18, 19, 20 and 21 and the estimation uncertainty in Fig. 22 it is possible to conclude that, the extension of PCA-based position sensor is able to estimate an accurate position, considering depth images with corrupted data until 50 % of ratio.

5.6 Global Stability with Wrong Initial Position and Attitude

The self-localization system stability is an important characteristic as it ensures that the estimator always converges to the real value for any initial condition. Considering that the proposed self-localization system is composed by two KF, the system global convergence is only achieved if each one is globally stable. For this purpose, three incorrect initial conditions for both position and attitude have been considered, as it is detailed in Table 1.

The results, depicted in Fig. 23, show that considering the incorrect initial conditions, the robot would follow, in open-loop, the same Lawn-Mower trajectory, but in a different direction. Considering these conditions, the position estimator could diverge from the robot real position. Figure 24 shows that KF results are always stable and exhibit fast convergence to the ground truth.

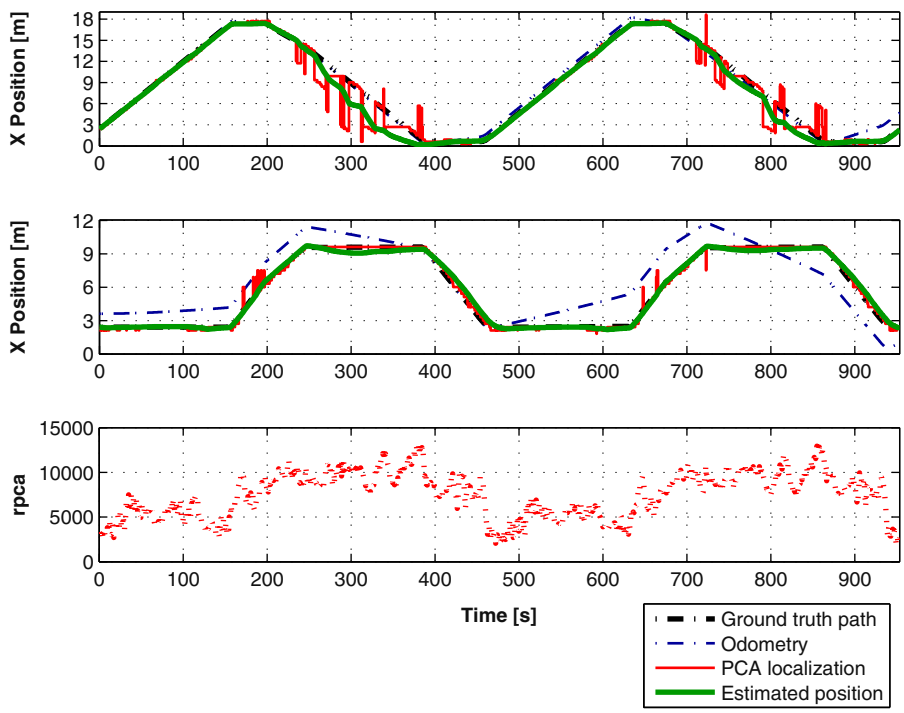

Fig. 27 Estimated position along time, searching in a neighborhood

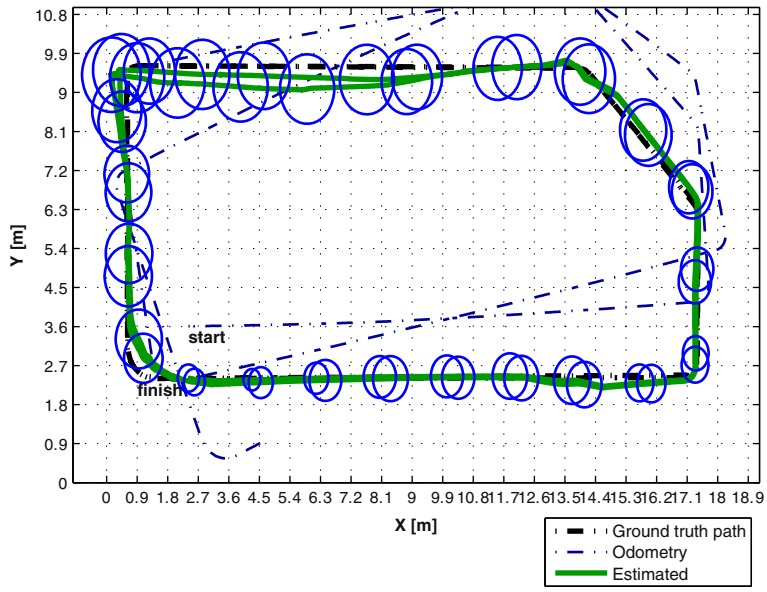

Fig. 28 Map with estimated position considering a ground truth path, searching in a neighborhood

5.7 2D Localization Results for a Longer Trajectory

After the validation of the proposed PCA-based self-localization system, considering depth images corrupted with missing data, another test is performed considering the motion of the robot in a large area and longer trajectories. Thus, a set of 1115 snapshots with depth images being captured in an area of 18.9 $m \times 9.6\ m$, considering the same grid map with a distance of 0.3 m and with the robot in the same attitude (see Fig. 5). The captured depth images are cropped with the same circular mask and sampled with a compression ratio of 100 : 1 and converted into a vector that will be added to the PCA eigenspace. Therefore, analyzing the corresponding PCA eigenvalues and selecting the same number of eigenvectors (30) of the previous experience, the selected components explain the images variability in an excess of 93 %. This corresponds to a reduction of 99.9 % in the memory resources when compared with the capacity needed to store the captured database, and 98.2 % when compared with the size after the subsample.

Once the physical structure of the environment when the test is performed is composed by equal equipments (pipes, air treatment units, light fixtures) distributed periodically along the ceiling, the mapping area incrementation to $18.9\ m \times 9.6\ m$, led the acquisition of similar images at different locations (Fig. 25). In consequence of the existence of periodic scenarios, when the PCA position sensor is comparing the eigenvector with all eigenspace, it is easily possible to find depth images, similar to the image captured during a mission, in a far localization. This causes large uncertainty in the position estimated by the PCA algorithm and, in consequence, in all self-localization system.

To solve the problem localization in scenarios with periodic elements, the searching considering a neighborhood δ around the mobile robot, proposed in (4) is applied. In the performed test, the neighborhood radius is variant and defined based on the eigenvectors distance obtained in last position estimation, through the linear relation $\delta = f_\delta \cdot r_{\text{PCA}}$. Considering the repeatability characteristics of the environment and the eigenvectors distance, the linear relationship is tunned to $f_\delta = 5 \times 10^{-4}$. This value ensures the searching of the nearest eigenvector in a radius between 1.5 m and 6.5 m around the mobile robot position estimated $\{\hat{x}(k), \hat{y}(k)\}$, as depicted in Fig. 26.

To test the mobile robot self-localization performance, considering periodic scenarios, several tests have been performed along a predefined path with length of 93 m, combining both straight lines and curves and traveling two laps inside the large mapped area, following the same method of the last experiments. Thus, the robot is moving with a speed of $0.1\ \text{m} \cdot \text{s}^{-1}$ and depth data is acquired with a 2.5 Hz of sampling rate and the real mobile robot trajectory is measured allowing the comparison of the estimated position with the real one (ground truth test).

Figures 27 and 28 present the results of the self-localization sensor, considering the PCA searching in a neighborhood, the KF position estimator and the real path of the robot, measured in the ground. The results of Fig. 27 show that the PCA is able to achieve an accurate position of the robot, allowing good performance on the global self-position sensor. Notice that the precision of the grid with depth images has 0.3 m of distance.

In Fig. 28 it is possible to see that the self-position sensor is able to converge the estimated position with the ground truth path while the odometry of the robot diverges completely from the real path. The blue circles represents the position uncertainty obtained by the Kalman filter. As it is possible to observe in Fig. 28, when the robot is in the top area, the uncertainty increases. The performance degradation occurs due to the fact that in this area the celling has less information. Nevertheless, Figs. 27 and 28 show that the robot is able to estimate its own position.

6 Conclusions

The existence of missing data in depth images is sometimes inevitable and it can induce a positioning system to an erroneous localization. In this paper an extension of a PCA methodology aiming to avoid the negative impact of missing data in signals has been developed and experimentally validated, allowing the follow advantages i) compression of the acquisition database; ii) corrupted data remotion in the depth image; and iii) and creation of new eigenvectors to compare the reconstructed depth image with the PCA database.

The proposed enhanced PCA-based localization system has been applied in a mobile robot localization system based on a Kinect sensor installed onboard, looking upwards to the ceiling, where the depth sensor often provides signals with missing data, caused by IR beams that not were reflected.

All tests were successfully performed, allowing to conclude that the proposed approach is useful in a number of mobile robotics applications where the existence of missing data is inevitable and causes a localization systems performance degradation. The robustness test allows to conclude that the proposed algorithm is able to estimate an accurate position, considering depth images with corrupt data ratio up to 50 %. The method has been tested in a environment with equal equipment installed periodically in the ceiling at different positions, causing repeatable scenarios in the acquired depth images during the robot missions. Searching for the closest vector in a neighborhood demonstrates the ability of PCA to be implemented in a system localization with environment repeatability. Moreover, the proposed method allows to validate the application of the Kinect depth sensor in a mobile robot localization system based on a extension of a classical PCA algorithm to operate in unstructured environments.

The integration of the PCA-based position sensor with linear Kalman filters allows to obtain an localization system and globally stable, under the Gaussian approach. The method was successfully validated in a self-localization system, using only onboard sensors and estimates the position with a global stable error dynamics.

In the future, the use of PCA for attitude estimation will be considered and implemented in the self-localization system, avoiding the use of the digital compass. As next step, the proposed localization method will be implemented in a path following control approach, where the self-localization system will be integrated in a control close loop. Later, in order to increase the self-knowledge about the place, the proposed PCA algorithm will be updated to create a dynamic PCA database. This development will allow an architecture able to perform different tasks like obstacle avoidance, robot-human interaction, rescue activities or integration in a multi-robots platform for collaborative work.

Acknowledgments The authors thank the valuable assistance of João Rodrigues in the development of the work reported in this paper.

This work was supported by FCT, through IDMEC, under LAETA Pest-OE/EME/LA0022 and partially supported by the project PRODUTECH-PTI (Proj. 3904) under the program COMPETE/QREN/FEDER.

References

1. Almansa-Valverde, S., Castillo, J.C., Fernndez-Caballero, A.: Mobile robot map building from time-of-flight camera. Expert Syst. Appl. **39**(10), 8835–8843 (2012). doi:10.1016/j.eswa.2012.02.006

2. Artač, M., Jogan, M., Leonardis, A.: Mobile robot localization using an incremental eigenspace model. In: Proceedings of ICRA 2002, the IEEE International Conference on Robotics and Automation, pp. 1025–1030. IEEE, Washington, DC (2002). doi:10.1109/ROBOT.2002.1013490
3. Bailey, T., Durrant-Whyte, H.: Simultaneous localization and mapping (SLAM): part II. Robotics Automation Magazine. IEEE **13**(3), 108–117 (2006). doi:10.1109/MRA.2006.1678144
4. Biswas, J., Veloso, M.: Depth camera based indoor mobile robot localization and navigation. In: Proceedings of ICRA 2012, the IEEE International Conference on Robotics and Automation, pp. 1697–1702. IEEE, Saint Paul (2012). doi:10.1109/ICRA.2012.6224766
5. Cardeira, C., Sá da Costa, J.: A low cost mobile robot for engineering education. In: Proceedings of IECON 2005, the 31st Annual Conference of the IEEE Industrial Electronics Society, pp. 2162–2167. Raleigh (2005). doi:10.1109/IECON.2005.1569239
6. Carreira, F., Christo, C., Valério, D., Ramalho, M., Cardeira, C., Calado, J.M.F., Oliveira, P.: 2d pca-based localization for mobile robots in unstructured environments. In: Proceedings of IROS 2012, the IEEE/RSJ International Conference on Intelligent Robots and Systems, pp. 3767–3868. IEEE, Vilamoura (2012). doi:10.1109/IROS.2012.6386272
7. Carreira, F., Christo, C., Valério, D., Ramalho, M., Cardeira, C., Calado, J.M.F., Oliveira, P.: Experimental validation of a PCA-based localization system for mobile robots in unstructured environments. IDMEC/CSI Internal Report (2012). http://www1.dem.ist.utl.pt/cardeira/Mesh/Ca12b.pdf
8. Carreira, F., Christo, C., Valério, D., Ramalho, M., Cardeira, C., Calado, J.M.F., Oliveira, P.: Experimental validation of a PCA-based localization system for mobile robots in unstructured environments. In: Proceedings of Robotica 2012, the 12th International Conference on Autonomous Robot Systems and Competitions, pp. 69–74. Guimarães (2012)
9. Carreira, F., Calado, J.M.F., Cardeira, C., Oliveira, P.: A bayesian grid method pca-based for mobile robots localization in unstructured environments. In: Proceedings of ICAR 2013, the 16th International Conference on Advanced Robotics. IEEE, Montevideo (2013)
10. Correa, D.SO., Sciotti, D.F., Prado, M.G., Sales, D.O., Wolf, D.F., Osório, F.S.: Mobile robots navigation in indoor environments using kinect sensor. In: Proceedings of CBSEC 2012, the 2nd Brazilian Conference on Critical Embedded Systems, pp. 36–41. IEEE, Campinas (2012). doi:10.1109/CBSEC.2012.18
11. Durrant-Whyte, H., Bailey, T.: Simultaneous localization and mapping: part I. Robotics automation magazine. IEEE **13**(2), 99–110 (2006). doi:10.1109/MRA.2006.1638022
12. Fukutani, Y., Takahashi, T., Iwahashi, M., Kimura, T., Salbiah, S.S., Mokhtar, N.B.: Robot vision network based on ceiling map sharing. In: Proceedings of AMC 2010, the 11th IEEE International Workshop on Advanced Motion Control, pp. 164–169. IEEE, Nagaoka (2010). doi:10.1109/AMC.2010.5464005
13. Ganganath, N., Leung, H.: Mobile robot localization using odometry and kinect sensor. In: Proceedings of ESPA 2012, the 1st IEEE International Conference on Emerging Signal Processing Applications, pp. 91–94. IEEE, Las Vegas (2012). doi:10.1109/ESPA.2012.6152453
14. Gil, A., Mozos, O., Ballesta, M., Reinoso, O.: A comparative evaluation of interest point detectors and local descriptors for visual slam. Mach. Vis. Appl. **21**, 905–920 (2010). doi:10.1007/s00138-009-0195-x
15. Huang, W., Tsai, C., Lin, H.: Mobile robot localization using ceiling landmarks and images captured from an rgb-d camera. In: Proceedings of AIM 2012, the IEEE/ASME International Conference on Advanced Intelligent Mechatronics, pp. 855–860. IEEE, Kachsiung (2012). doi:10.1109/AIM.2012.6265979
16. Jo, S., Choi, H., Kim, E.: Ceiling vision based slam approach using sensor fusion of sonar sensor and monocular camera. In: Proceedings of ICCAS 2012, the 12th International Conference on Control, Automation and Systems, pp. 1461–1464. IEEE, Kuala Lumpur (2012)
17. Jolliffe, I.: Principal Component Analysis. Springer-Verlag (2002). doi:10.1007/b98835
18. Kröse, B., Bunschoten, R., Hagen, S.T., Terwijn, B., Vlassis, N.: Household robots look and learn: environment modeling and localization from an omnidirectional vision system. IEEE Robot. Autom. Mag. **11**, 45–52 (2004). doi:10.1109/MRA.2004.1371608
19. Kuo, B.W., Chang, H.H., Chen, Y.C., Huang, S.Y.: A light-and-fast slam algorithm for robots in indoor environments using line segment map. J. Robot. **2011**, 257852 (2011). doi:10.1155/2011/257852
20. Larsson, U., Forsberg, J., Wernersson, A.: Mobile robot localization: integrating measurements from a time-of-flight laser. IEEE Trans. Ind. Electron. **43**(3), 422–431 (1996). doi:10.1109/41.499815
21. Maohai, L., Han, W., Lining, S., Zesu, C.: Robust omnidirectional mobile robot topological navigation system using omnidirectional vision. Eng. Appl. Artif. Intel. **26**(8), 1942–1952 (2013). doi:10.1016/j.engappai.2013.05.010
22. Oliveira, P.: MMAE terrain reference navigation for underwater vehicles using PCA. Int. J. Control. **80**(7), 1008–1017 (2007). doi:10.1080/00207170701242515
23. Oliveira, P., Gomes, L.: Interpolation of signals with missing data using principal component analysis. Multidim. Syst. Signal Process **21**(1), 25–43 (2010). doi:10.1007/s11045-009-0086-3
24. Scaramuzza, D., Fraundorfer, F., Siegwart, R.: Real-time monocular visual odometry for on-road vehicles with 1-point ransac. In: Proceedings of ICRA 2009, the IEEE International Conference on Robotics and Automation, pp. 4293–4299. IEEE, Kobe (2009). doi:10.1109/ROBOT.2009.5152255
25. Siagian, C., Itti, L.: Biologically inspired mobile robot vision localization. IEEE Trans. Robot. **25**(4), 861–873 (2009). doi:10.1109/TRO.2009.2022424
26. Stowers, J., Hayes, M., Bainbridge-Smith, A.: Altitude control of a quadrotor helicopter using depth map from microsoft kinect sensor. In: Proceedings of ICM 2011, the IEEE International Conference on Mechatronics, pp. 358–362. IEEE, Istanbul (2011). doi:10.1109/ICMECH.2011.5971311

27. Theodoridis, T., Hu, H., McDonald-Maier, K., Gu, D.: Kinect enabled monte carlo localisation for a robotic wheelchair. In: Frontiers of Intelligent Autonomous Systems, vol. 466, pp. 17–27. Springer (2013). doi:10.1007/978-3-642-35485-4_2
28. Thrun, S., Burgard, W., Fox, D.: Probabilistic Robotics. Intelligent Robotics and Autonomous Agents. MIT Press (2005)
29. Turk, M., Pentland, A.: Eigenfaces for recognition. J. Cogn. Neurosci. **3**(1), 71–86 (1991). doi:10.1162/jocn.1991.3.1.71
30. Xu, D., Han, L., Tan, M., Li, Y.F.: Ceiling-based visual positioning for an indoor mobile robot with monocular vision. IEEE Transactions on Industrial Electronics **56**(5), 1617–1628 (2009). doi:10.1109/TIE.2009.2012457